



Particle-based solar thermochemical and thermal energy storage

Peter G. Loutzenhiser

Solar Fuels and Technology Laboratory

Woodruff School of Mechanical Engineering

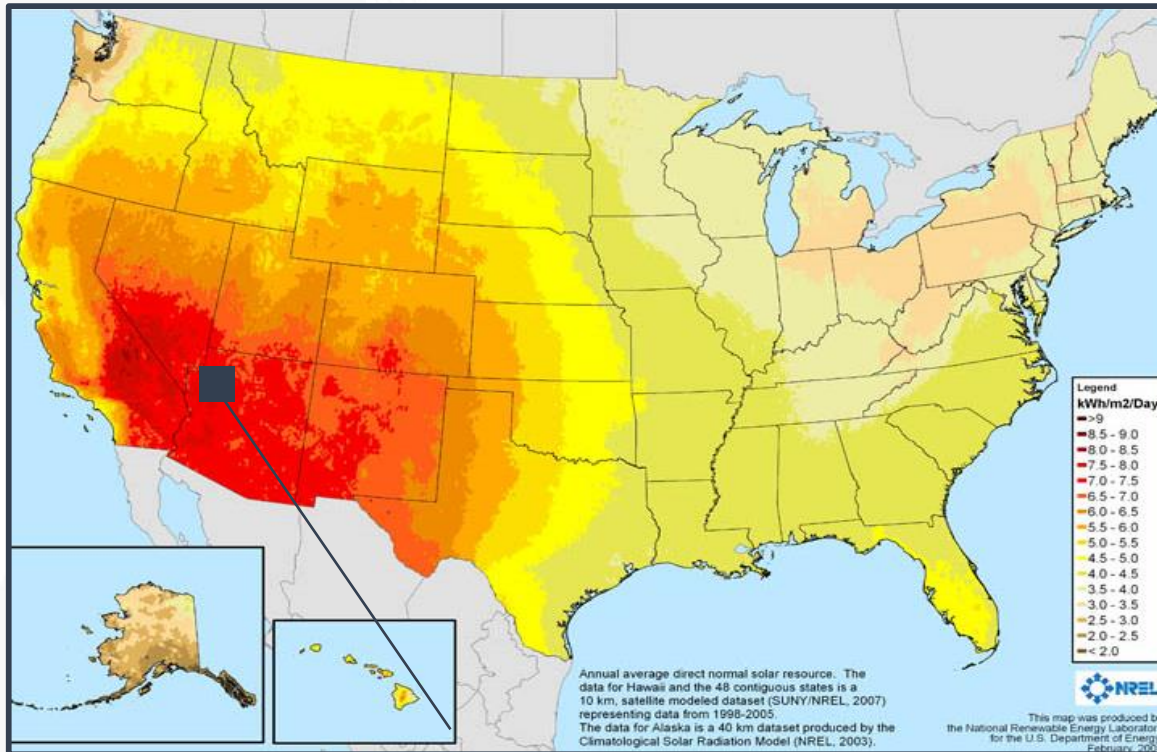
Thermal-Mechanical-Chemical Electricity Storage

Workshop

February 4, 2020

Solar potential and limitations

Annual solar irradiation in the United States



Limitations of Solar Energy

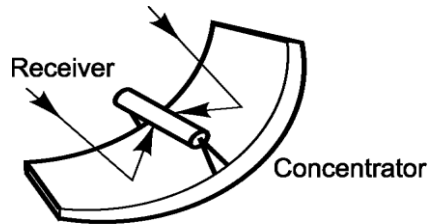
- **Dilute:** Maximum direct-normal solar irradiance of $1 \text{ kW}\cdot\text{m}^{-2}$
- **Intermittent:** Solar energy can only be harvested when the sun is shining
- **Unequally distributed:** Optimal areas for harvesting solar energy are near the equator away from population centers

10% conversion to a usable form of energy in an area $126 \times 126 \text{ km}^2$ could have supply all the energy needs in the United States

Concentrating solar irradiation

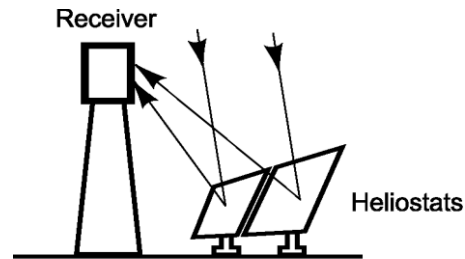
Trough

Solar concentrations
of < 100 suns



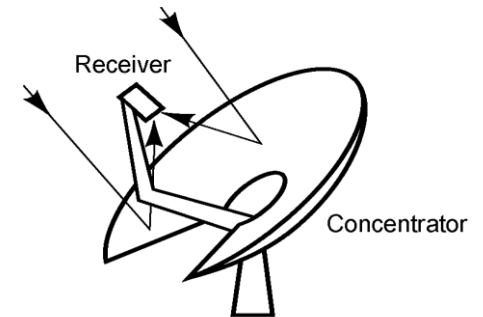
Tower

Solar concentrations
of 500 – 2500 suns
with secondary



Dish

Solar concentrations
of 5000 – 10,000 suns



Maximum work potential extraction

$$\eta_{\text{overall,ideal}} = \eta_{\text{absorption}} \eta_{\text{Exergy}} = \underbrace{\left(1 - \frac{\sigma T^4}{I_{\text{DN}} C}\right)}_{\frac{\dot{Q}_{\text{solar}} - \dot{Q}_{\text{re-radiation}}}{Q_{\text{solar}}}} \cdot \underbrace{\left(1 - \frac{T_{\text{ambient}}}{T}\right)}_{\text{theoretical work potential from heat (exergy)}}$$

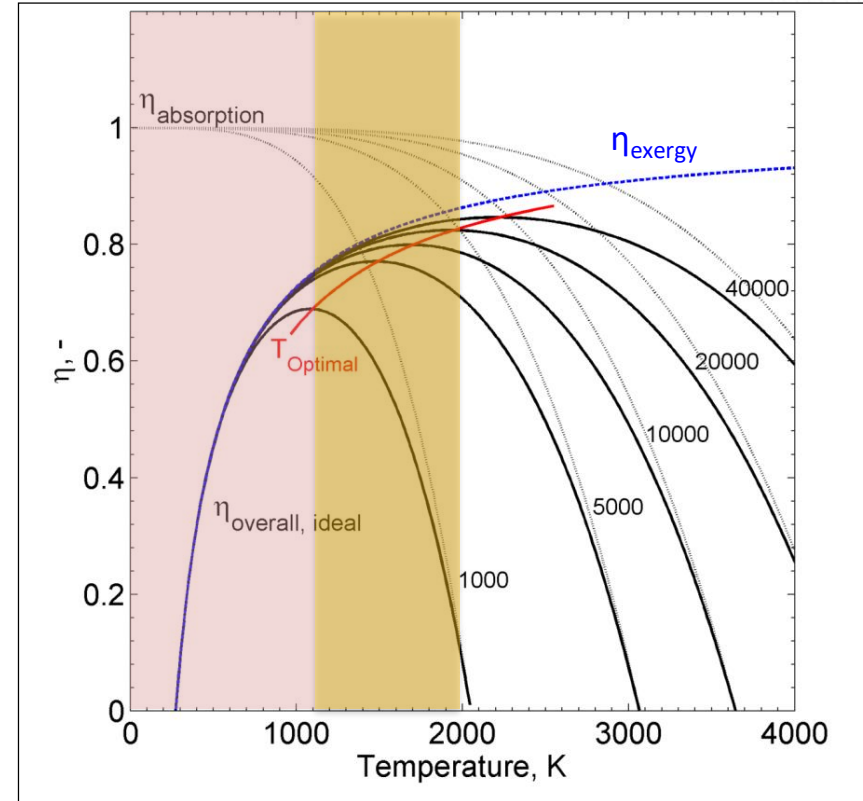
$$\eta_{\text{overall,ideal}} = 0 \rightarrow T_{\text{stagnation}} = \left(\frac{I_{\text{DN}} C}{\sigma}\right)^{0.25}$$

$$\frac{\partial \eta_{\text{overall,ideal}}}{\partial T_{\text{optimal}}} = 0$$

$$0 \rightarrow (T_{\text{optimal}})^5 - 3/4 T_{\text{ambient}} (T_{\text{optimal}})^4 - \left(\frac{T_{\text{ambient}} I_{\text{DN}} C}{4\sigma}\right) = 0$$

C	1000 suns	5000 suns	10000 suns
$T_{\text{stagnation}}$	2049 K	3064 K	3644 K
T_{optimum}	1106 K	1507 K	1724 K

nuclear range
ideal thermochemical cycles



Sensible thermal energy storage media molten salts

Advantages

- ❖ Relatively inexpensive
- ❖ High energy density
- ❖ Low vapor pressures
- ❖ Discharges at constant conditions

Disadvantages

- ❖ High melting points (~200 °C Solar Salt)
- ❖ Low thermal conductivities
- ❖ Relatively low temperatures of stability (~585 °C Solar Salt)
- ❖ Relatively hard to pump and corrosive

Thermal and thermochemical energy storage with particles

Advantages

- ❖ Directly irradiated
- ❖ Low-cost, abundant media (e.g. sand, casting media)
- ❖ Higher operating temperatures/efficiency
- ❖ Existing bulk transport, storage technologies
- ❖ Various receiver configurations available

Sensible thermal energy storage media

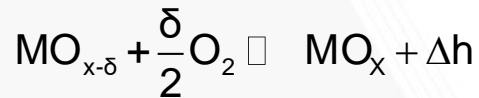
- ❖ High thermal capacitance
- ❖ High solar absorptance
- ❖ Enhanced heat transfer due to small particles

Thermochemical storage media

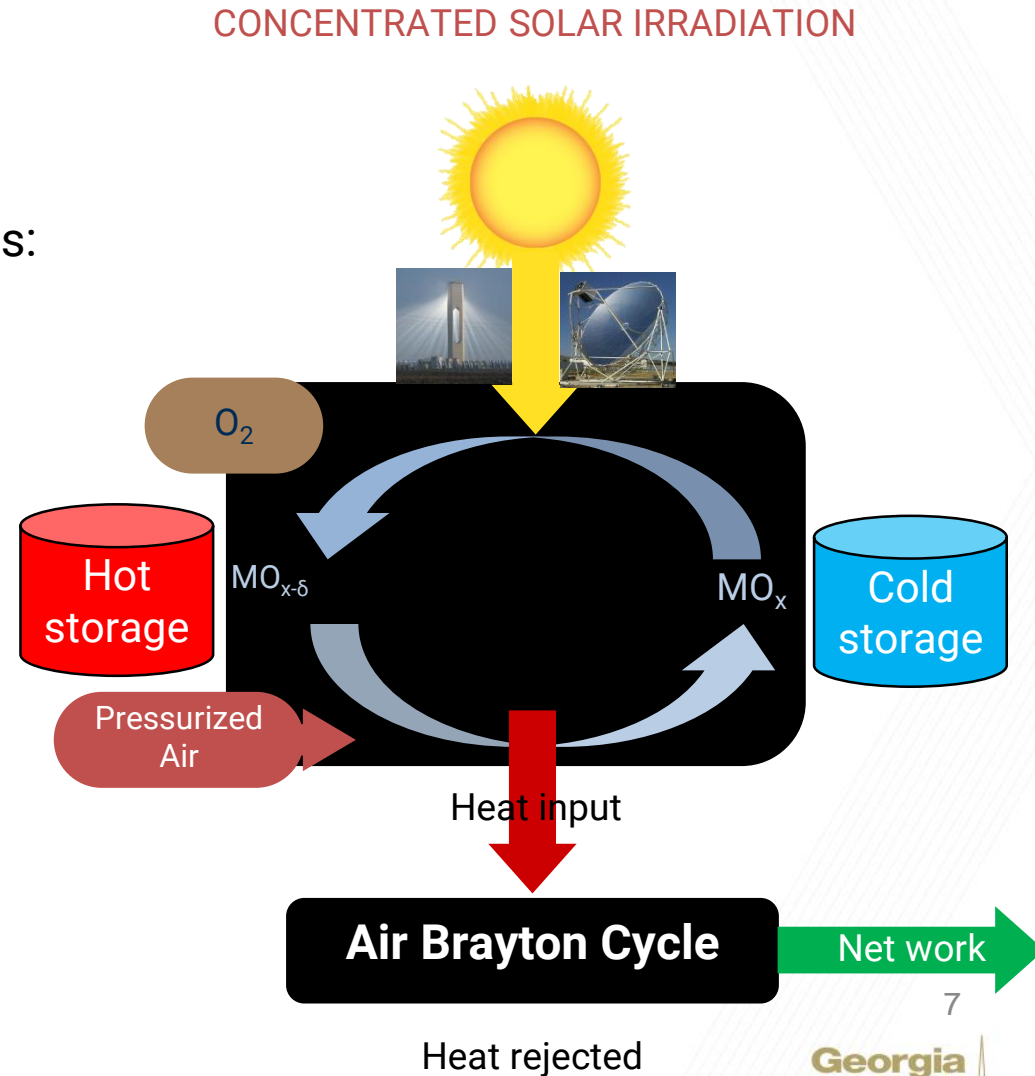
- ❖ Increased energy power densities
- ❖ Maintains higher temperatures during the exothermal release of heat

Solar thermochemical heat storage concept for integration into an Air Brayton cycle

- ❖ Solar thermochemical energy storage via a two-step solar thermochemical cycle for integration in an Air Brayton cycle based off of redox-active materials:

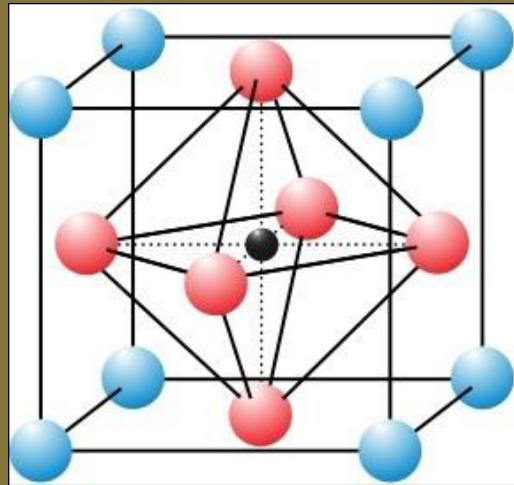


- ❖ Enables heat storage in both a chemical and sensible form
- ❖ The added chemical storage increases the energy densities of the material to better account for intermittency of sunlight



Design constraints for solar receiver

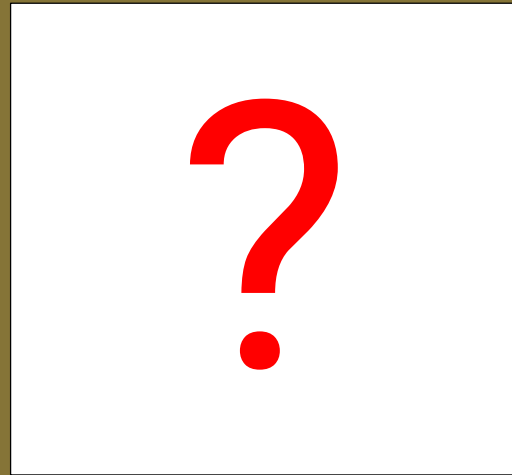
Redox-active materials development



Cation substitution to “tune” MIEC materials for

- ❖ Increased redox capacitance and reaction enthalpy
- ❖ Faster kinetics from increased oxygen mobility
- ❖ Optimized thermodynamics
- ❖ CAM28 particles

Thermochemical reactor development

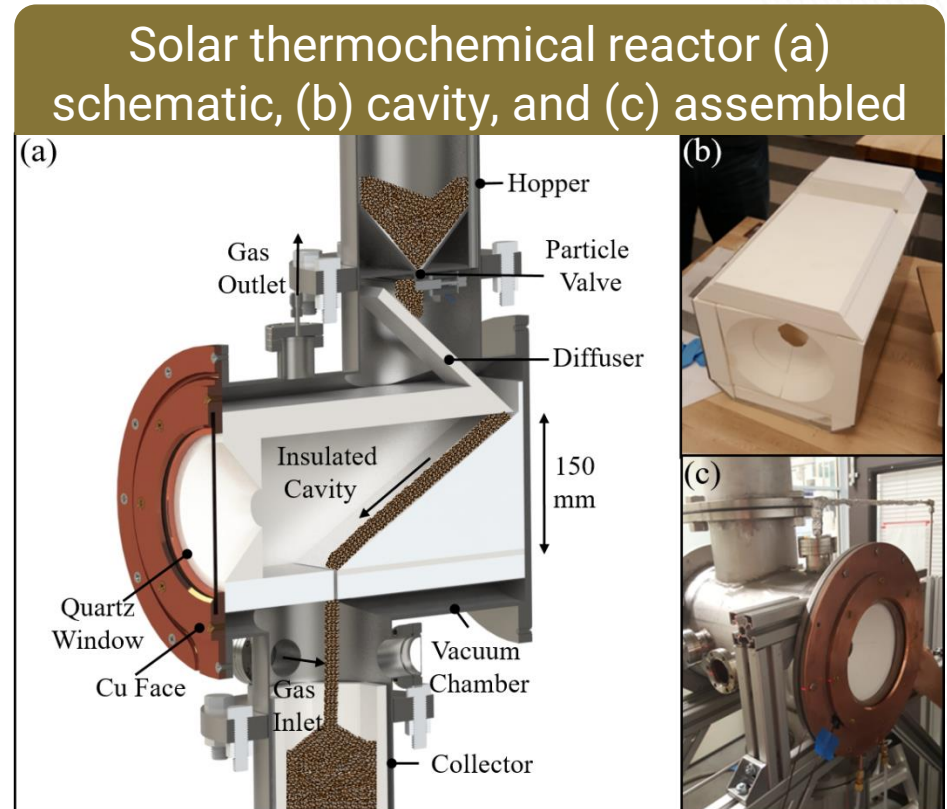


Thermochemical reactors must also be designed for

- ❖ Optimal absorption of concentrated solar irradiation
- ❖ Specific solar concentrating facilities
- ❖ Redox-active materials and residence times

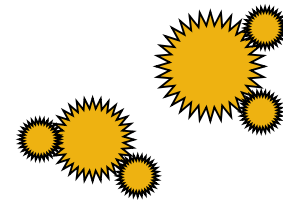
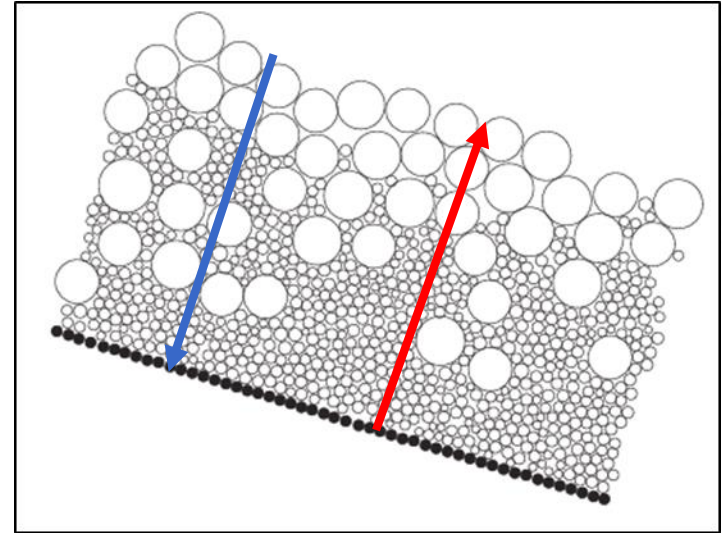
5 kW_{th} Solar Thermochemical Inclined Granular-Flow Reactor (STInGR)

- ❖ Thermochemical energy storage of solar energy within a dense, granular flow of reactive particles
- ❖ Aluminosilicate insulated cavity inserted within steel, cylindrical vacuum chamber
- ❖ Reactor sealed using steel flanges, hopper / collector cylindrical assemblies, quartz window
- ❖ Incident irradiation introduced through quartz window using HFSS, concentrated on 40 mm diameter aperture
- ❖ Residence time controlled by variable inclination angle, mass flow rate, slope roughness
- ❖ Reactor capable of receiving various granular media, specifically tuned for $\text{CaAl}_{0.2}\text{Mn}_{0.8}\text{O}_{3-\delta}$

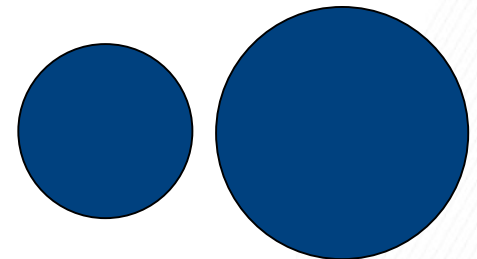


Granular flow theory

- ❖ Bulk transport influenced by competing time scales
 - Inter-particle contact time versus $\left(\frac{\partial u}{\partial z}\right)^{-1}$
- ❖ Bulk transport sensitive to development of small population of long-lived contacts
 - Electrostatic forces
 - Cohesion
 - Particle shape, size interactions
 - Soft particles
 - Temperature effects (e.g., particle softening, agglomeration, thermophoresis)



**Jagged shapes
susceptible to
long-lived
contacts**



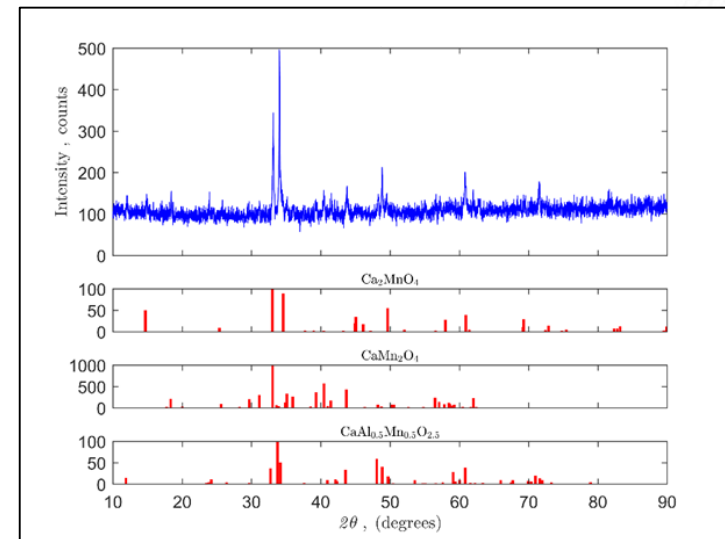
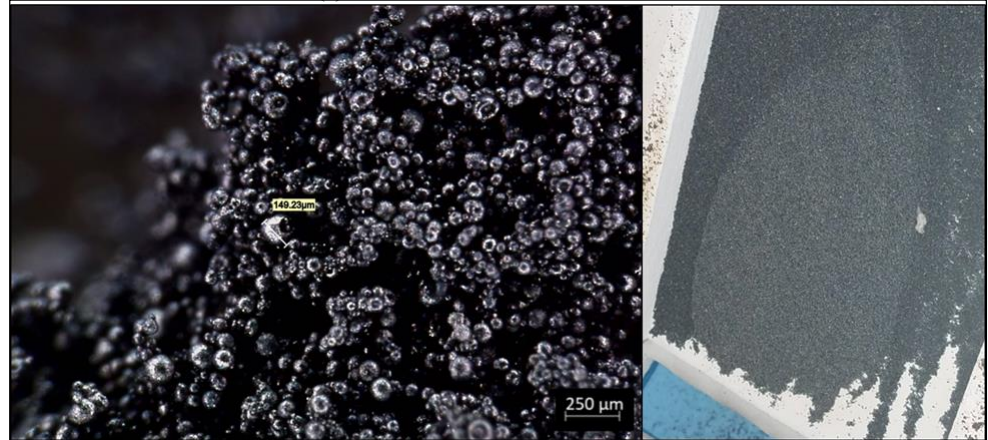
**Spherical shapes
susceptible to binary
particle interactions**

Experimental results from solar reactor

- ❖ Severe agglomeration of CAM28 powders observed to occur at $T > 900$ °C.
- ❖ Agglomeration observed at similar temperatures for high-density spray-dried calcium manganites with common impurities used in chemical looping combustion.
- ❖ Common impurities of spray-dried calcium manganites observed in XRD analysis of materials.

Peak intensities from X-ray diffraction for (top) Coorstek particles cycled repeatedly through the 5 kWth reactor during high flux solar simulator experimentation and (bottom) for potential phase impurities Ca_2MnO_4 , CaMn_2O_4 , and $\text{CaAl}_{0.2}\text{Mn}_{0.8}\text{O}_{2.5}$ samples

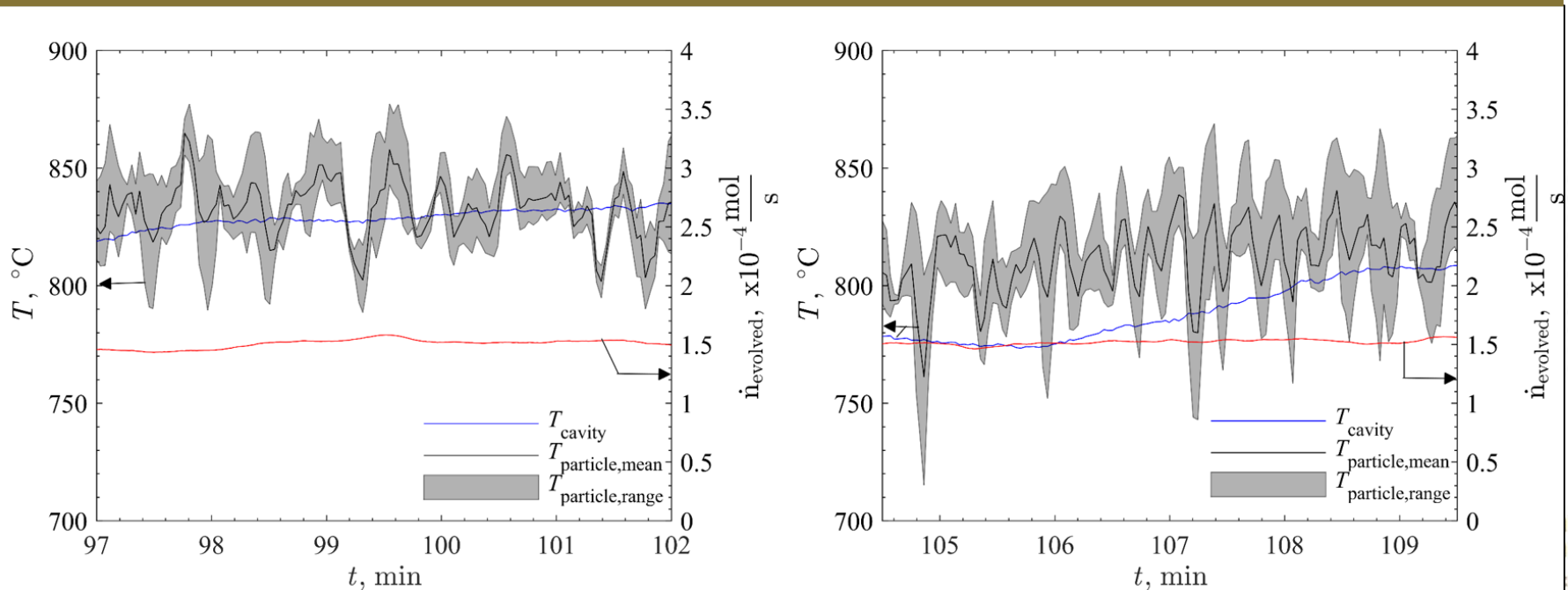
Agglomerates from as viewed by optical microscopy (left) and along the slope (right)



Experimental performance

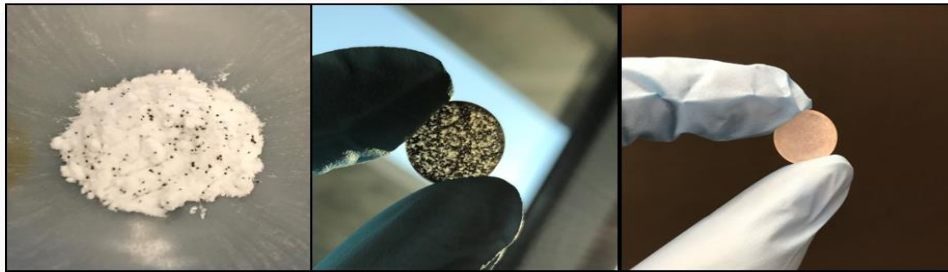
- ❖ Severe agglomeration avoided if $\bar{T} < 875$ °C.
- ❖ Replicated steady state experiments performed with $\dot{Q}_{\text{HFSS}} = 2.7 \text{ kW}_{\text{th}}$ with HFSS lamps 2-6.
- ❖ $\bar{T}_{\text{outlet}} = 830 - 850$ °C, $\overline{\Delta\delta}_{\text{outlet}} = 0.012$, $\eta_{\text{th}} = 0.785$
- ❖ η_{th} greater than anticipated due to lower T and higher \dot{m}_{CAM28}

Temporal temperature (cavity and particulate) and O₂ measurements



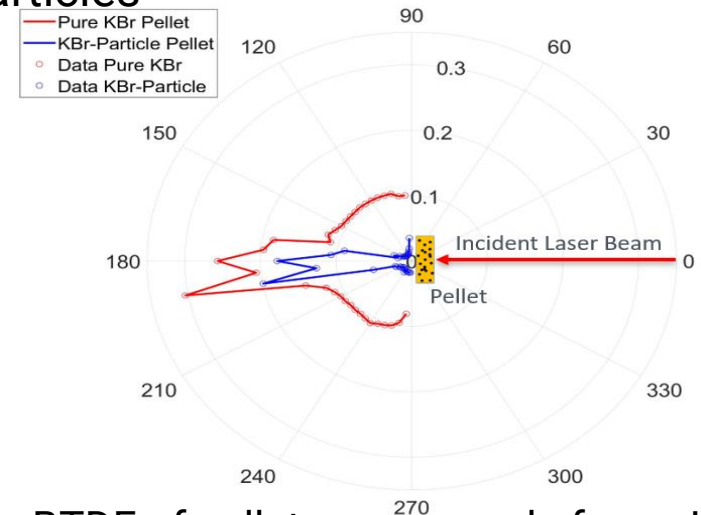
Characterization of scattering phase function setup/measurements

- ❖ Three Axis Automated Scatterometer (TAAS)
- ❖ Requires particle-KBr pellet
- ❖ Laser wavelength: 635 nm
- ❖ Pellet fabrication parameters
- ❖ 13 mm diameter, ~ 7 ton load compaction, no vacuum, powder pulverized



Fabrication of the KBr pellet with particles: (left) a mixture of KBr powder and ID50 particles; (middle) the 1% by weight KBr-particle pellet after compression; (right) a pure KBr pellet for reference

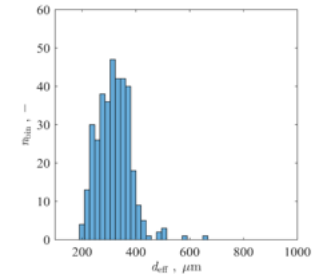
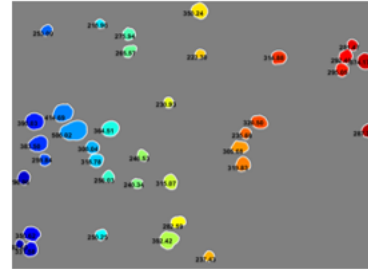
- ❖ Bi-directional Transmittance Distribution Function (BTDF)
- ❖ Preliminary results indicate strong forward scattering normal to pellet
- ❖ Similar pattern observed for both pellets, uniform decrease due to particles



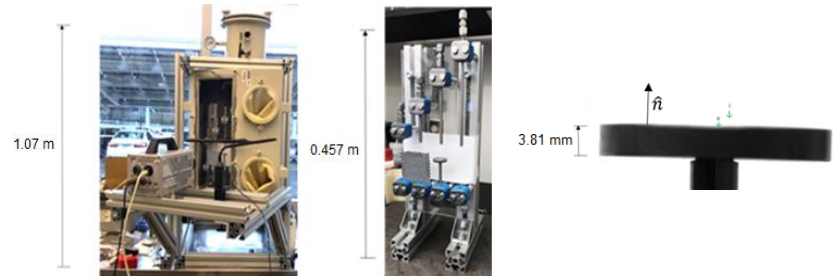
BTDF of pellets composed of pure KBr powder (red) and KBr-particle mixtures of 1 wt% particles (blue)

Characterization of mechanical properties up to 800 °C

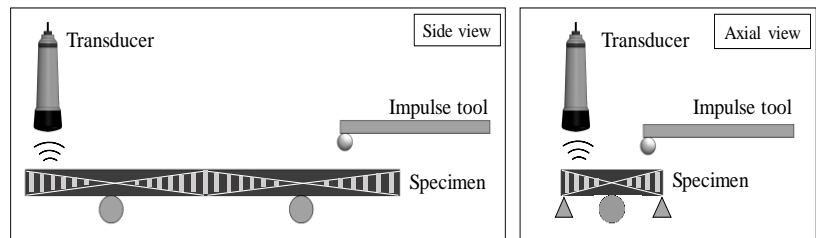
Developed a program to determine particle size distributions and roundness



Modified a vacuum chamber coupled to a high-speed camera to measure coefficient of restitution



Developing protocols with impulse excitation tests to determine modulus of elasticity and Poisson's ratio



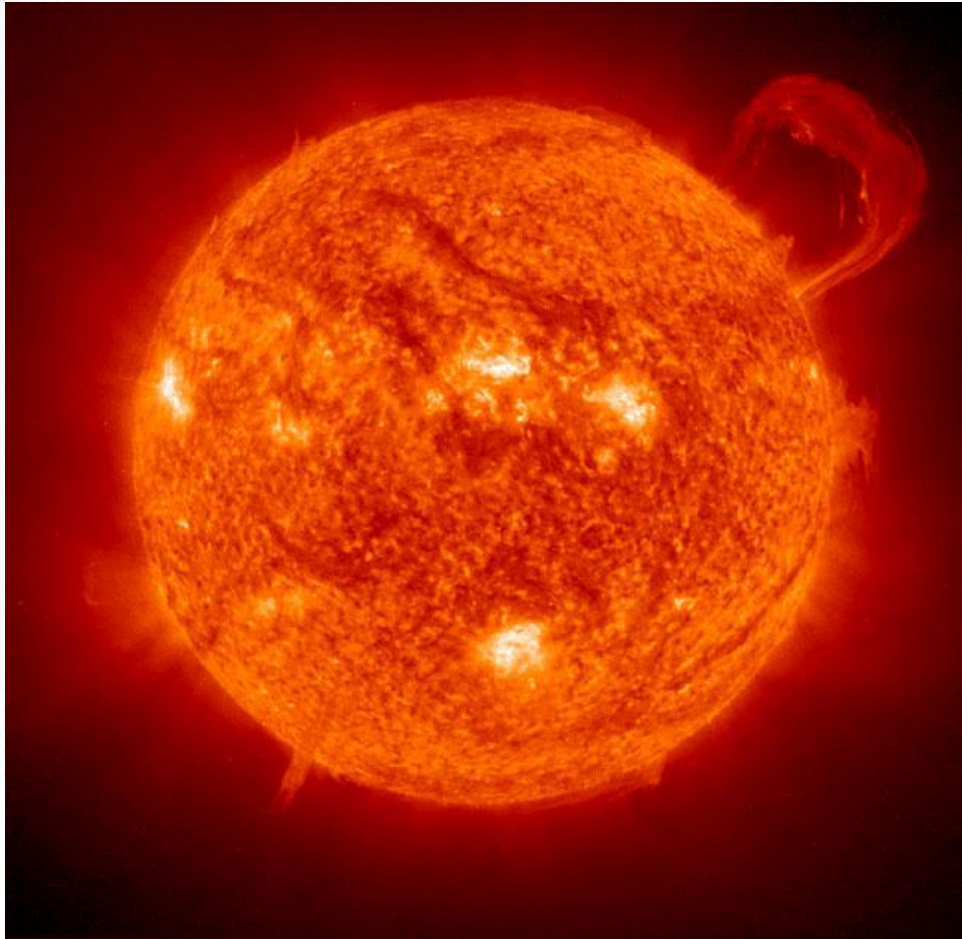
Developing a slip-stick apparatus to measure static and dynamic coefficients of friction

Conclusions and summary

- ❖ Particulate (granular) flows are excellent solar thermal energy storage media for reaching elevated temperatures and higher solar-to-electric efficiencies
- ❖ Redox-active particles for thermochemical energy storage media increase the overall power densities of the materials and allow for long-term storage
- ❖ Material properties need to be accurately characterized to design the next generation of particle heating receivers/reactors

Outlook

How does the future look?



Acknowledgements

- ❖ Funding from the Solar Energy Technologies Office: DE-EE0008372 with project oversight provided by Drs. Matthew Bauer and Andru Prescod (SETO)
- ❖ Funding: U.S. Department of Energy SunSHOT initiative under Award No. DE-FOA-0000805-1541 (PROMOTES project in ELEMENTS) with project oversight from Levi Irwin (SETO)
- ❖ National Science Foundation Graduate Research Fellowship under Grant No. DGE-1148903
- ❖ Graduate Research Assistants: Malavika Bagepalli, H. Evan Bush, Chuyang Chen, Robert Gill, Alexander Muroyama, Andrew Schrader, Garrett Schieber, and Justin Yarrington
- ❖ Collaborators:
 - ❖ Georgia Tech: Devesh Ranjan, Zhuomin Zhang, Sheldon Jeter
 - ❖ Arizona State University: James Miller, Ellen Stechel, Nathan Johnson
 - ❖ King Saud University: Hany Al-Ansary
 - ❖ Sandia National Laboratories: Andrea Ambrosini, Sean Babiniec, Cliff Ho, and James Miller